JOURNAL OF GEOPHYSICAL RESEARCH, VOL. 113, B01405, doi:10.1029/2007JB004927, 2008

Spatiospectral localization of global geopotential fields from the Gravity Recovery and Climate Experiment (GRACE) reveals the coseismic gravity change owing to the 2004 Sumatra-Andaman earthquake

Shin-Chan Han[1,2] and Frederik J. Simons[3,4]

Received 3 January 2007; revised 22 August 2007; accepted 5 November 2007; published 23 January 2008.

[1] Regional mass fluxes owing to transport and adjustment within the Earth system that are implicitly contained in the monthly Gravity Recovery and Climate Experiment (GRACE) global geopotential coefficients are revealed by localizing global spectra using spatiospectrally concentrated window functions. We have analyzed 45 monthly global GRACE harmonic coefficient series in order to find the coseismic signature associated with the 2004 great Sumatra-Andaman earthquake. A significant gravity change after the earthquake is found in the time series of the GRACE coefficients after localization with a single band-limited window centered near the north of the island of Sumatra. This change is undetectable from the original global coefficients or from coefficients localized elsewhere on the globe. A step function with its discontinuity at 26 December 2004 usefully models the coseismic gravity change. The localized GRACE coefficients contain the jumps (associated with the earthquake) up to degree and order 55, although not all of them within this band produce changes that are statistically significant. The gravity change calculated from the localized GRACE coefficients displays 30 μGal peak-to-peak variations that are very well correlated with an independently derived seismic model based on elastic dislocation theory.

Citation: Han, S.-C., and F. J. Simons (2008), Spatiospectral localization of global geopotential fields from the Gravity Recovery and Climate Experiment (GRACE) reveals the coseismic gravity change owing to the 2004 Sumatra-Andaman earthquake, *J. Geophys. Res.*, *113*, B01405, doi:10.1029/2007JB004927.

1. Introduction

[2] The motion of Earth-orbiting satellites is governed primarily by spatial and temporal variations of Earth's gravity field. The Gravity Recovery and Climate Experiment (GRACE) satellite mission has been providing valuable data that reflect both mass distribution and redistribution within the Earth system by detecting the changes in distance between two proof masses, identical satellites orbiting Earth at 500 km mean altitude. Since their launch in March 2002, extensive analyses of time-variable gravity have resolved hydrological mass fluxes across large river basins [*Tapley et al.*, 2004b], global mean ocean mass variations [*Chambers et al.*, 2004], ocean tides [*Ray et al.*, 2003], ice sheet mean mass fluxes [*Luthcke et al.*, 2006; *Velicogna and Wahr*, 2006], and solid-Earth mass movements and density changes [*Han et al.*, 2006], to name but a few applications of this remarkable and growing data set. The global spherical harmonic (SH) analysis of the GRACE satellite tracking data has been the principal approach to generate monthly mean geopotential fields [*Tapley et al.*, 2004a]. Instrumental and other system errors yield a theoretical limit on the accuracy of the solutions. Additional modeling errors, such as aliasing errors [*Han et al.*, 2004] require special processing in order to approach this limit. Various spatial smoothing techniques have been developed to mitigate errors in the ill-determined SH coefficients at higher degree and order [*Wahr et al.*, 1998; *Davis et al.*, 2004; *Han et al.*, 2005; *Swenson and Wahr*, 2006; *Kusche*, 2007]. All of those postprocessing techniques are to be applied to the monthly mean gravity field maps or SH coefficients, the so-called level 2 (L2) products.

[3] Spherical harmonics are nonlocalized, global spherical basis functions [*Freeden and Michel*, 1999] and the effective bandwidth of SH expansions of typical smoothing windows grows fast in response to the progressive restriction of such windows to spatial regions of interest as a result of the Heisenberg uncertainty principle [*Percival and Walden*, 1993]. Independently from the GRACE community, a method to constrain regional contributions to global SH spectra has been developed in the context of planetary tectonics [*Simons et al.*, 1997] and used to detect the incomplete

[1]Planetary Geodynamics Laboratory, NASA Goddard Space Flight Center, Greenbelt, Maryland, USA.
[2]Also at Goddard Earth Science and Technology Center, University of Maryland, Baltimore County, Baltimore, Maryland, USA.
[3]Department of Earth Sciences, University College London, London, UK.
[4]Now at Department of Geosciences, Princeton University, Princeton, New Jersey, USA.

0148-0227/08/2007JB004927$09.00

rebound of the Canadian Laurentide ice sheet [*Simons and Hager*, 1997]. The windows constructed by this method were axisymmetric and obeyed a useful but ad hoc criterion to achieve a balance between spatial and spectral concentration. *Wieczorek and Simons* [2005] quantified the concentration criterion and derived by optimization the shape of ideally concentrated but still isotropic window functions.

[4] The principle is simple. Seeking a band-limited function that is optimally concentrated within a spherical cap extending over the colatitudes $0 \leq \theta \leq \theta_0$ amounts to maximizing the ratio of the energy of the function within the region compared to the entire sphere. We denote this ratio

$$\lambda = \int_0^{2\pi}\int_0^{\theta_0} h^2(\theta)\sin\theta d\theta d\varphi \Big/ \int_0^{2\pi}\int_0^{\pi} h^2(\theta)\sin\theta d\theta d\varphi, \quad (1)$$

where θ is colatitude, φ is longitude, and $h(\theta)$ is an azimuthally invariant window given by the band-limited zonal SH expansion

$$h(\theta) = \sum_{l=0}^{L_h} h_l Y_{l0}(\Omega), \quad (2)$$

where Y_{l0} is a properly normalized real spherical harmonic of degree $0 \leq l \leq L_h$ and order $m = 0$ on the unit sphere $\Omega = (\theta, \varphi)$ (see *Wieczorek and Simons* [2005] for further details). The desired coefficients h_l are found by diagonalizing a square and symmetric "localization kernel," as follows:

$$\sum_{l'=0}^{L_h} D_{ll'} h_{l'} = \lambda h_l, \quad (3)$$

where the elements $D_{ll'}$ are integrals of products of Legendre functions. These can be computed accurately by numerical integration, or, in the axisymmetric polar cap case, analytically without great effort [*Simons et al.*, 2006; *Simons and Dahlen*, 2006]. In that case, they define a matrix that is tridiagonal, which lends itself easily to diagonalization.

[5] *Simons et al.* [2006] extended the above ideas to nonaxisymmetric windows optimally concentrated within an arbitrarily shaped boundary. Their methods are expected to be well-suited for the analysis of time-variable gravity fields from GRACE since each of the time-variable signals appears only associated with its own particular geographical regime and usually displays characteristic temporal behavior and intensity. Time-dependent geophysical signals tend to originate in geographically confined regions, while satellite measurement errors are relatively uniformly distributed over the globe. At the same time, the noise affecting individual SH geopotential coefficients grows significantly with increasing degree, and thus care must be taken to limit the bandwidth of any localizing window so as to minimize spectral leakage effects. By localizing the global SH fields to the area (spatially as well as within the appropriate spectral range) where the signal is expected to appear with most of its energy, the signal-to-noise ratio (SNR) can be significantly enhanced.

[6] An earthquake-triggered gravity change exemplifies perfectly the type of phenomenon that is better analyzed by spatiospectral localization since its power attenuates rapidly away from the epicenter and thus results primarily in regional anomalies. The great Sumatra-Andaman earthquake ($M_w > 9.0$) on 26 December 2004 ruptured the seafloor by several to tens of meters along the Java/Sunda trench (over 1300 km in length) within 7–8 min [*Ammon et al.*, 2005]. It permanently changed Earth's gravity field [*Sabadini et al.*, 2005] and disturbed the distance between the two GRACE satellites, normally separated by approximately 220 km. These minute changes in intersatellite distance were measured with the onboard K-band microwave ranging (KBR) instrument [*Tapley and Reigber*, 2005]. *Han et al.* [2006] studied the coseismic deformation near the subduction zone from the satellite-tracking data directly (thus not from the L2 products of the global SH modeling) and documented, for the first time, evidence for crustal dilatation as a result of the Sumatra-Andaman earthquake.

[7] In this study, we show the power of the localization method of *Wieczorek and Simons* [2005] in unlocking observational evidence of the Sumatra-Andaman earthquake directly from the L2 monthly time series of GRACE global SH geopotential coefficients. The intuitive ease by which the method affords the extraction of geophysical signal by postprocessing of the L2 solutions should be welcomed by the science community at large. We show that the coseismic gravity changes processed from the monthly global fields are resolved with almost the same spatial resolution as the regional inversion method [*Han et al.*, 2006] that, however, requires greater efforts. We quantify how large the effects of the earthquake are in the time series of individual SH harmonic coefficients after windowing. These measurements are subsequently analyzed on the basis of a seismic model based on elastic dislocation theory [*Okada*, 1992; *Okubo*, 1992] by considering various effects such as the vertical displacements of the seafloor and Moho topography, expansion of the crust and compression of the mantle.

2. Localization of Global Geopotential Fields

[8] We have used 45 monthly GRACE SH coefficient sets sensitive to the monthly mean geopotential field (these are unconstrained solutions from the Center for Space Research, Release 01; *Tapley et al.* [2004a]) spanning the interval from August 2002 to July 2006. (Those data are available from the website http://podaac.jpl.nasa.gov/grace.) Unlike *Tapley et al.* [2004b], we do not smooth by spatial convolution to reduce undesired effects caused by higher-degree (l) and -order (m) coefficients ($l, m \geq 15$), which are characterized by poor SNR. Rather, we focus on a specific region by applying an optimal windowing function or taper to the time series of GRACE gravity maps in the spatial domain or, equivalently, by performing an equivalent procedure on the time series of GRACE SH coefficients in the spectral domain. We refer to either of those operations as "spatiospectral localization."

[9] Briefly explained, the original geophysical signal, $f(\theta, \varphi)$, will be given by the expansion

$$f(\theta,\varphi) = \sum_{l=0}^{\infty}\sum_{m=-l}^{l} f_{lm} Y_{lm}(\Omega), \quad (4)$$

and its inverse

$$f_{lm} = \frac{1}{4\pi} \int_{\Omega} f(\Omega) Y_{lm}(\Omega) d\Omega. \quad (5)$$

The spatially windowed signal, $\Phi(\theta, \varphi) = h(\theta)f(\theta, \varphi)$, however, will have expansion coefficients

$$\Phi_{lm} = \frac{1}{4\pi} \int_{\Omega} h(\theta) f(\Omega) Y_{lm}(\Omega) d\Omega. \quad (6)$$

The spectral-domain equivalent to equation (6) is to obtain Φ_{lm} from the original f_{lm} (the L2 product) by an operation reminiscent of a convolution:

$$\Phi_{lm} = \sum_{l'} H_{ll'} f_{l'm}, \quad (7)$$

where the "coupling" between the original coefficients at degrees l' and the windowed coefficients at degree l is described by the matrix whose elements $H_{ll'}$ are contained in the work of *Wieczorek and Simons* [2005, equation (10)]. They involve the quantum-mechanical Wigner 3*j* symbol that is readily evaluated numerically; the summation limits in equation (7) are determined by selection rules [*Dahlen and Tromp*, 1998]. The important feature of equation (7) is that the coupling is confined to at most twice the bandwidth L_h of the localizing window $h(\theta)$ of equation (2), which we take to be a number small enough that the optimization of equation (1) yields one well-concentrated basis function for which $\lambda \approx 1$. The localized field coefficients thus capture geophysical signal that arises from the target geographical area (a "polar cap" rotated to the desired location) but they also have the advantage of being narrow-band smoothed renderings of the global coefficients. This enhances the SNR of the regional geophysical signal compared to the unfiltered global expansion coefficients.

[10] The spatiospectral localization of the global spectra suppresses errors (and signals) originating from outside of the region of interest. The suppression of the errors is typically greater than that of the signal if the signal is intense only within the region of interest where the localization window is applied. Consequently the localization improves SNR of the local signal contained in the global spectra. This way of processing the satellite gravity estimates is fundamentally different from the ones based on spatial smoothing over the globe that has been used widely in the community. The spatiospectral localization may be better suited to investigate mass variation associated with localized geophysical phenomena.

[11] In this paper, we use a single band-limited (maximum expansion degree of $L_h = 15$) window function, $h(\theta)$, that is isotropic and maximally concentrated within a spherical cap with a radius of $\theta_0 = 25°$ centered around 5°N, 95°E. No band-limited function can be strictly space-limited [*Simons et al.*, 2006]. Thus the analysis window is globally defined but its energy is optimally concentrated within our region of interest. The spatial concentration criterion that is optimized is the ratio of the energy of the window function within the spherical cap with respect to the entire globe as in equation (1). The band-limited window function is to be determined such that the concentration ratio λ is maximized. This concentration problem can be reformulated in the spectral domain, upon which it eventually amounts to finding the eigenvalues (the concentration ratios) and eigenvectors (the band-limited set of SH coefficients of a family of window functions) of a tridiagonal matrix whose elements are determined by the size of the spherical cap (θ_0) and the maximum degree of the SH expansion of the window function (L_h), as outlined in section 1 (see *Wieczorek and Simons* [2005] for more details). In an alternative formulation of the problem, exactly space-limited window functions can be found whose SH spectrum is not band-limited but maximally concentrated within the band. These window functions are identical to ours within the domain of the spherical cap (i.e., for $\theta \leq \theta_0$) and their SH expansions agree to within a scaling factor inside of the band (i.e., for $l, m \leq L_h$).

[12] Figure 1a illustrates the window function, concentrated within a spherical cap with radius $\theta_0 = 25°$ and band-limited to a maximum degree and order $L_h = 15$. The concentration ratio (λ i.e., the eigenvalue of the tridiagonal diagonalization problem) exceeds 0.999, that is, less than 0.1% of the identified signal will originate from outside the region of interest. To show the oscillatory behavior outside the cap clearly, the evaluated function values are scaled by a factor of 100 when the radius is greater than θ_0. Each of the monthly GRACE SH solutions was convolved, in the manner suggested by equation (7), with the coupling matrix of the window function rotated to various locations, in the Amazon (5°S, 295°E), the North Pacific (20°N, 195°E), and Sumatra (5°N, 95°E). The 45 monthly time series of the original and windowed GRACE SH coefficients were used to compute the root-mean-squared energy per degree (the degree-RMS) every month and the time-averaged degree-RMS was computed from the 45 monthly degree-RMS curves. The degree-RMS as a measure of the total field strength (square root of power) of each spectral degree is defined as follows:

$$S(l) = \sqrt{\sum_{m=0}^{l} C_{lm}^2 + S_{lm}^2}, \quad (8)$$

where C_{lm} and S_{lm} are the cosine and sine SH coefficients of the original or windowed GRACE fields. Figure 1b shows the time-averaged degree-RMS of the original and the windowed GRACE solutions at various locations. The plot shows that the original GRACE spectra are overwhelmed by measurement errors when the degree exceeds 15–20. After windowing, the overall strength of the windowed fields (including both the signal and noise) is suppressed by up to one order of magnitude, depending on their location (the areas are identical) and the spectral regime (either of signal or error). The field windowed about the center of the Amazon contains more prevailing power in the low degrees ($l < 25$) than the other two regions, which is readily attributed to the large seasonally dominated temporal gravity changes reflecting the Amazonian hydrological cycle [*Tapley et al.*, 2004b]. The other extreme is in the center of the North Pacific, where GRACE is expected to detect the least temporal variability. The field windowed

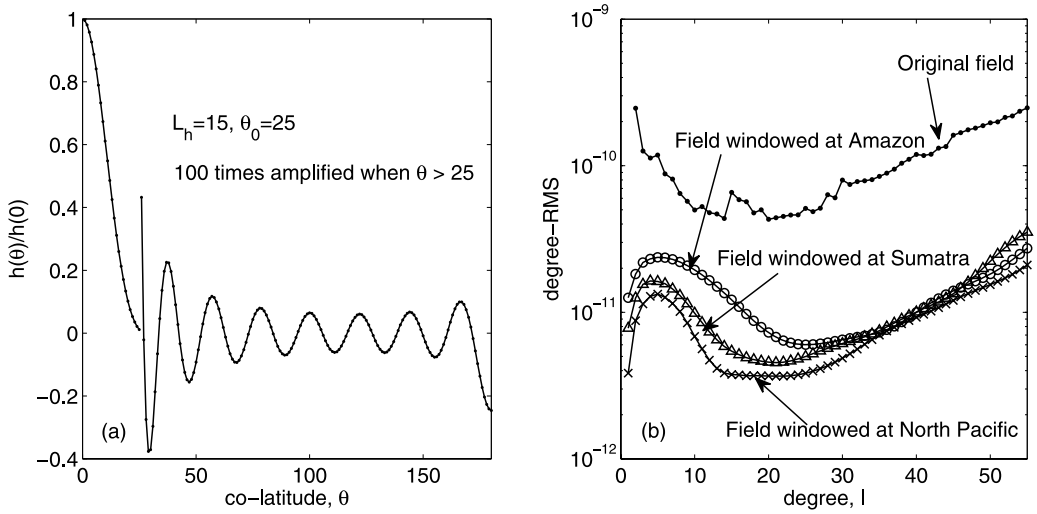

Figure 1. (a) The optimal zonal window function with spectrum band-limited to spherical harmonic degree and order $L_h = 15$. It is maximally concentrated within a spherical cap with a radius of $\theta_0 = 25°$. There are oscillations outside the cap (out of our region of interest) with approximately 100 times smaller magnitude. The concentration ratio (i.e., the ratio of the energy of the window within the cap ($\theta \leq \theta_0$) to the whole-sphere energy) is greater than 0.999. Note that the plot shows the function scaled by a factor 100 when the spherical distance is greater than 25°. (b) Time-averaged root-mean-squared energy per degree (degree-RMS) of the temporal variations from the 45 monthly GRACE geopotential fields. In Figure 1b, we applied to the original field the window function centered at various locations: Amazon (5°S/295°E), Sumatra Island (5°N/95°E), and the North Pacific (20°N/195°E).

about this point in the North Pacific shows the least power in the low degrees. Our primary interest is the windowed field north of the island of Sumatra, close to the epicenter of the 26 December 2004 great Sumatra-Andaman earthquake, which is characterized by a degree-RMS that lies in between that of the Amazon and Pacific regions. The fields windowed at those three different locations contain very similar amounts of power in the noise regime ($l > 25$). Thus, while the strength of the time-variable signals varies depending on the geographical location, the contribution owing to noise remains relatively stationary across the globe. It is immediately obvious that applying the data window enhances the relative contribution of the local signal of the gravity variations owing to mass redistribution with respect to the global noise: i.e., we eventually enhance the SNR by windowing.

[13] In Figure 2, we show the calculated spatial distribution of the mean gravity variations over 45 months before (Figures 2a–2c) and after (Figures 2d–2f) windowing in the region around Sumatra (shown by the circles). The time-averaged root-mean-squared strength (RMS) of the 45 monthly changes is shown up to maximum SH degrees of 15, 25, and 55 for Figures 2a and 2d, Figures 2b and 2e, and Figures 2c and 2f, respectively, as indicated by the legends. The RMS maps from expansions truncated at 15 and 25 in Figures 2a and 2b reveal signal that is predominantly large over the continents. However, the RMS of the gravity variations truncated at 55 in Figure 2c is dominated by errors. We applied the window function and focus on the variability in our region of interest, which is depicted in (d), (e) and (f). The effects of signal and noise from outside the spherical cap are strongly suppressed even if they are not completely zero.

3. Stepwise Patterns in the Time Series of the Windowed GRACE Coefficients

[14] The effect of windowing in the space domain is roughly equivalent to convolution in the spectral domain. The effect of this convolution-like operation on a certain coefficient with a degree l results in a linear combination of the neighboring SH coefficients inside the band between $l - L_h$ and $l + L_h$, whereby L_h is the bandwidth of the data window, as shown by *Simons et al.* [1997] and *Wieczorek and Simons* [2005]. This spectral smoothing suppresses the effect of random noise on the original SH coefficients at the cost of decreasing the spectral resolution. The maximum SH degree and order of the windowed field that can be studied without truncation effect is reduced to $L - L_h$, when L is the maximum degree and order of the original fields. We use the GRACE fields up to degree and order 70 and thus we examine the windowed coefficients to 55 given the window's bandwidth of $L_h = 15$. Examples of the time series of GRACE SH coefficients are given in Figures 3–5.

[15] A subset of the results that we will analyze and interpret hereafter appears in Figure 3. They are the time series of windowed coefficients (C_{lm} and S_{lm}) for various degrees and orders (l and m) as shown in the legend. The windows used are centered on the epicenter of the great 2004 Sumatran-Andaman earthquake. The time series of windowed coefficients have been offset in this figure by amount that yields a geoid height of 0 μm geoid variation in December 2004, to facilitate inspection. For comparison,

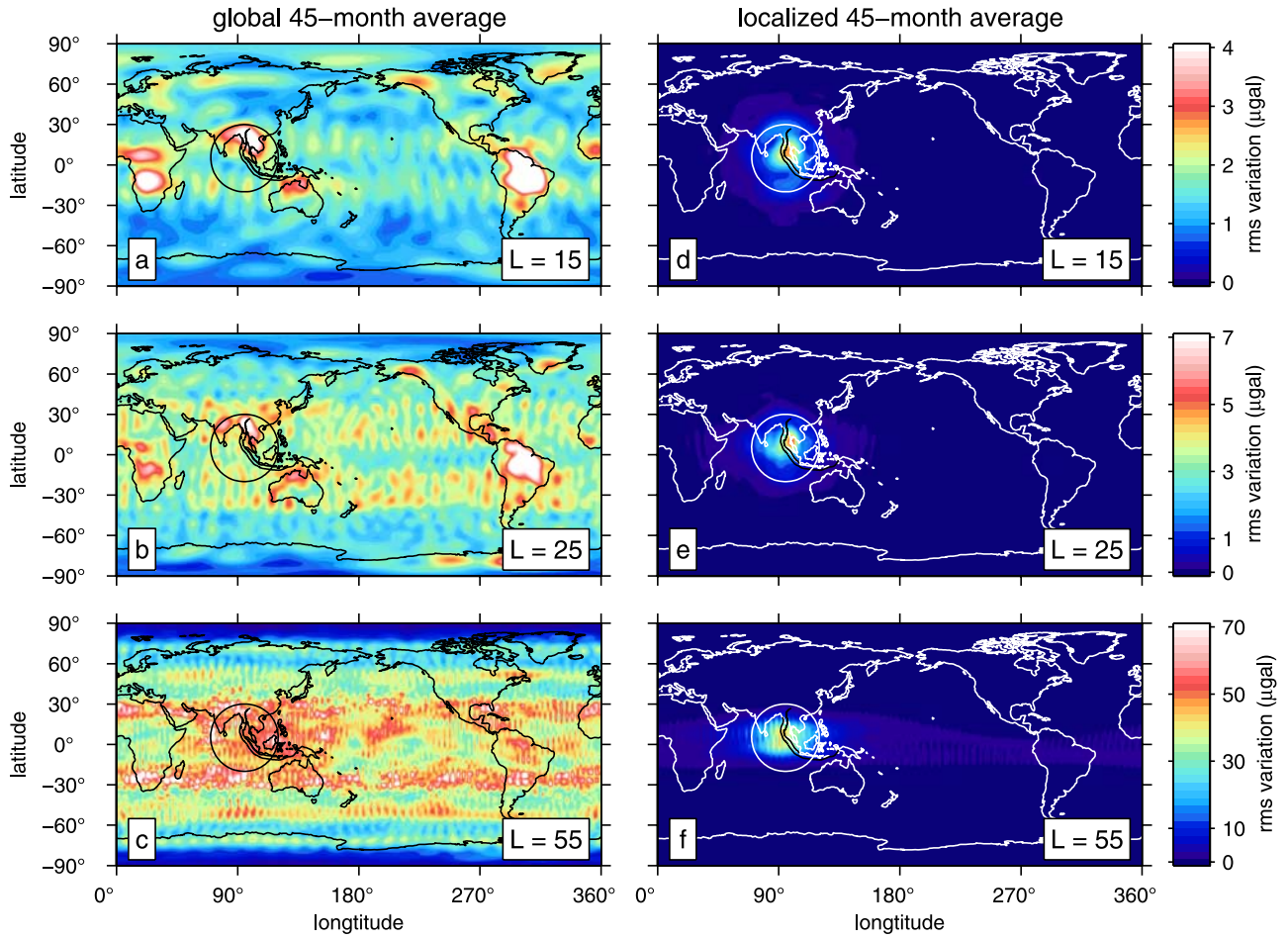

Figure 2. Root-mean-square strength of the temporal gravity variations (in μGal) from 45 monthly GRACE geopotential fields up to degree and order (a) 15, (b) 25, and (c) 55. (d–f) The same as (a–c), respectively, but after applying the window function shown in Figure 1a centered at 5°N/95°E. In this figure and others to follow, we show the location of the Java trench, the Andaman ridge, and the Sumatra and Sagaing transform faults in addition to the continental outlines.

Figure 4 shows time series, at identical degrees and orders, of the original, unwindowed solutions. In the analysis that is to follow, it will be nearly impossible to distill any meaningful information out of these unprocessed L2 products. Finally, Figure 5 shows time series of the l = 26, m = 8 cosine and sine coefficients after tapering with a window whose center shifts progressively off target. As expected, the geophysical signal that we interpret below to be associated with the Sumatran-Andaman earthquake is gradually lost as the distance of the window to the epicenter increases.

[16] Three analytic models were fitted to each of the time series. The first model (M1) includes a static offset as well as annual and semiannual sinusoids with which we attempt to explain seasonal signals. The second model (M2) uses the same parameterization as the first one with one additional parameter for a linear trend to account for interseasonal or secular change. In the third model (M3), we introduced to M1 a step function on 26 December 2004 in order to quantify an abrupt change in the gravity before and after the 2004 great Sumatra-Andaman earthquake. The step occurs between December 2004 and January 2005 since GRACE solutions are monthly means. After least-squares fitting of the three models to each of the time series, we determined whether the parameters inverted for are significant in the time series on the basis of a t test. We consider either the linear trend or the stepwise pattern to be well

Figure 3. Time series of the tapered GRACE geopotential coefficients (C_{lm} in the left column and S_{lm} in the right column) after applying the window function centered at 5°N in latitude and 95°E in longitude (gray triangles). The examples shown are for various degrees and orders l/m = 4/4, 19/1, 26/8, 32/20, 43/14, and 52/25. The least squares fits to the GRACE time series are shown by black circles. The annual and semiannual sinusoids, a linear trend, and a step function with discontinuity at the 2004 Sumatra-Andaman earthquake event have been considered for the least-squares modeling and statistical t tests have been performed to find significant parameters. There are significant discontinuities implying coseismic change found in many of the localized coefficients. The variance reduction (vr; in %) for each of the fits is shown.

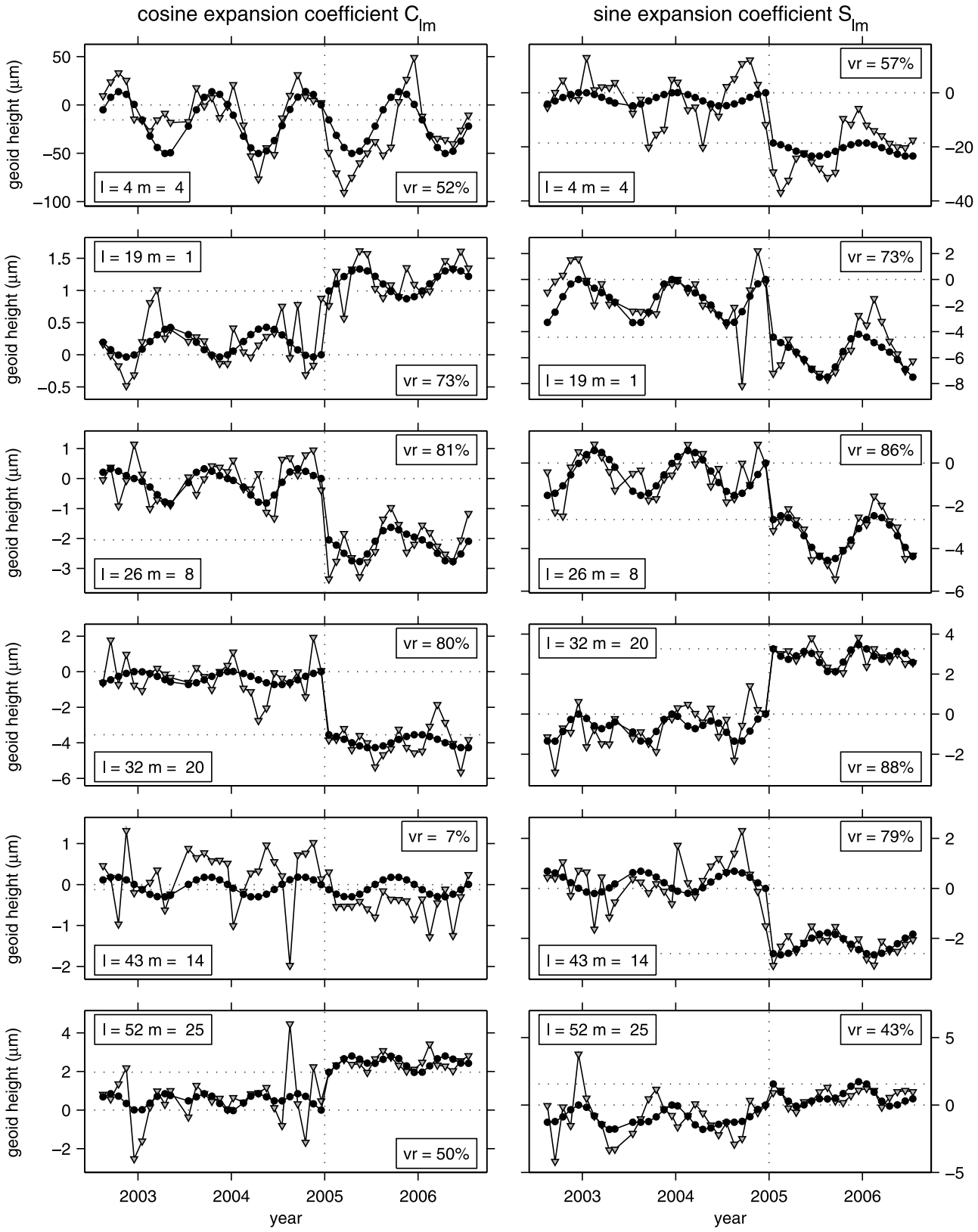
cosine expansion coefficient C_{lm}
sine expansion coefficient S_{lm}
geoid height (μm)
l = 4 m = 4
vr = 52%
vr = 57%
l = 19 m = 1
vr = 73%
vr = 81%
l = 26 m = 8
vr = 86%
vr = 80%
l = 32 m = 20
vr = 88%
vr = 7%
l = 43 m = 14
vr = 79%
l = 52 m = 25
vr = 50%
vr = 43%
2003
2004
2005
2006
year

Figure 3

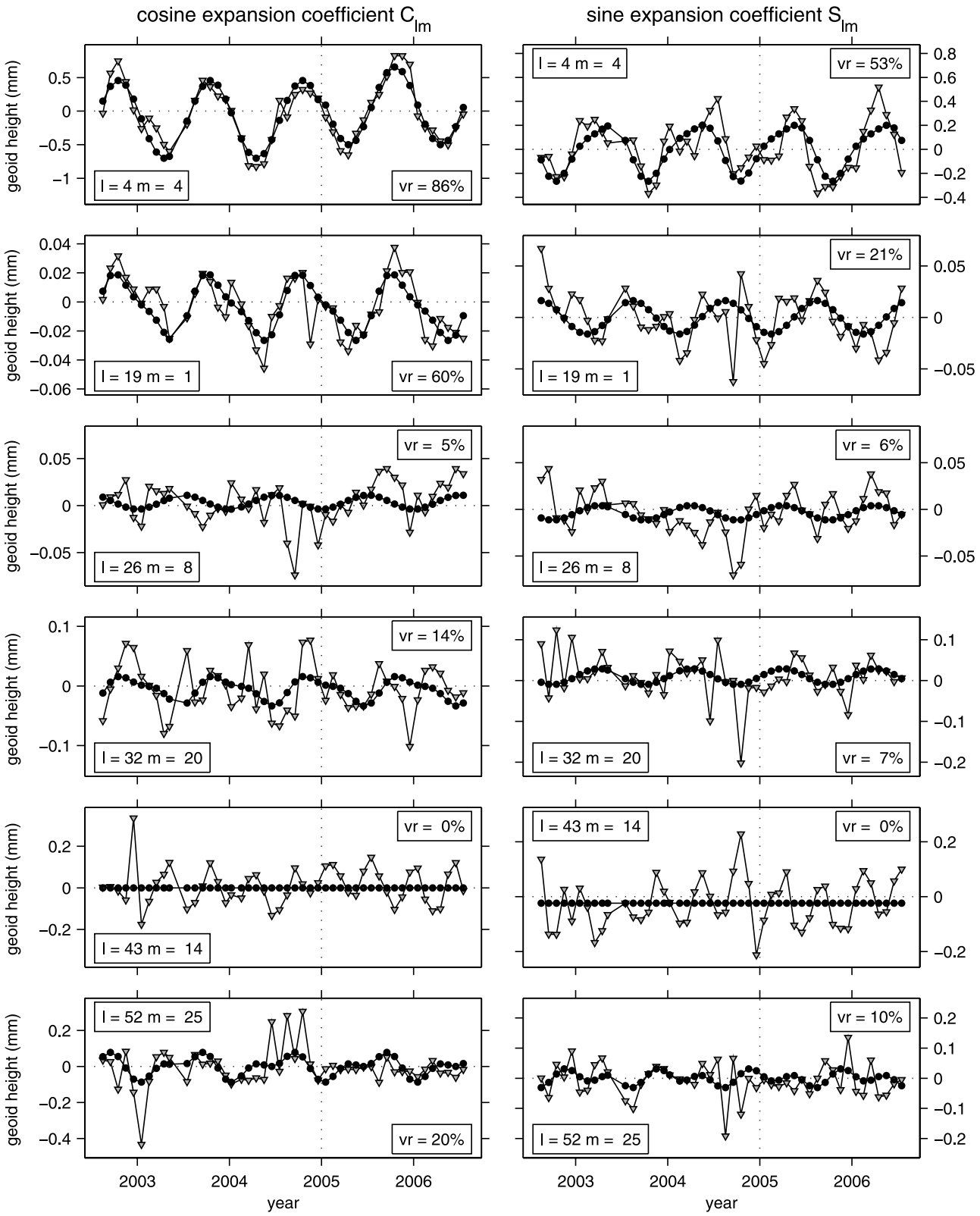

Figure 4. Time series of the original GRACE geopotential coefficients (C_{lm} and S_{lm}) at various degrees and orders; l/m = 4/4, 19/1, 26/8, 32/20, 43/14, and 52/25. The same least-squares fit and statistical tests have been conducted as in Figure 3, and the same symbols are used in both figures. The fits are shown with solid dots. The straight lines in the time series of $C_{43,14}$ and $S_{43,14}$ indicate that there is no statistically significant parameter that could be fitted to the observations.

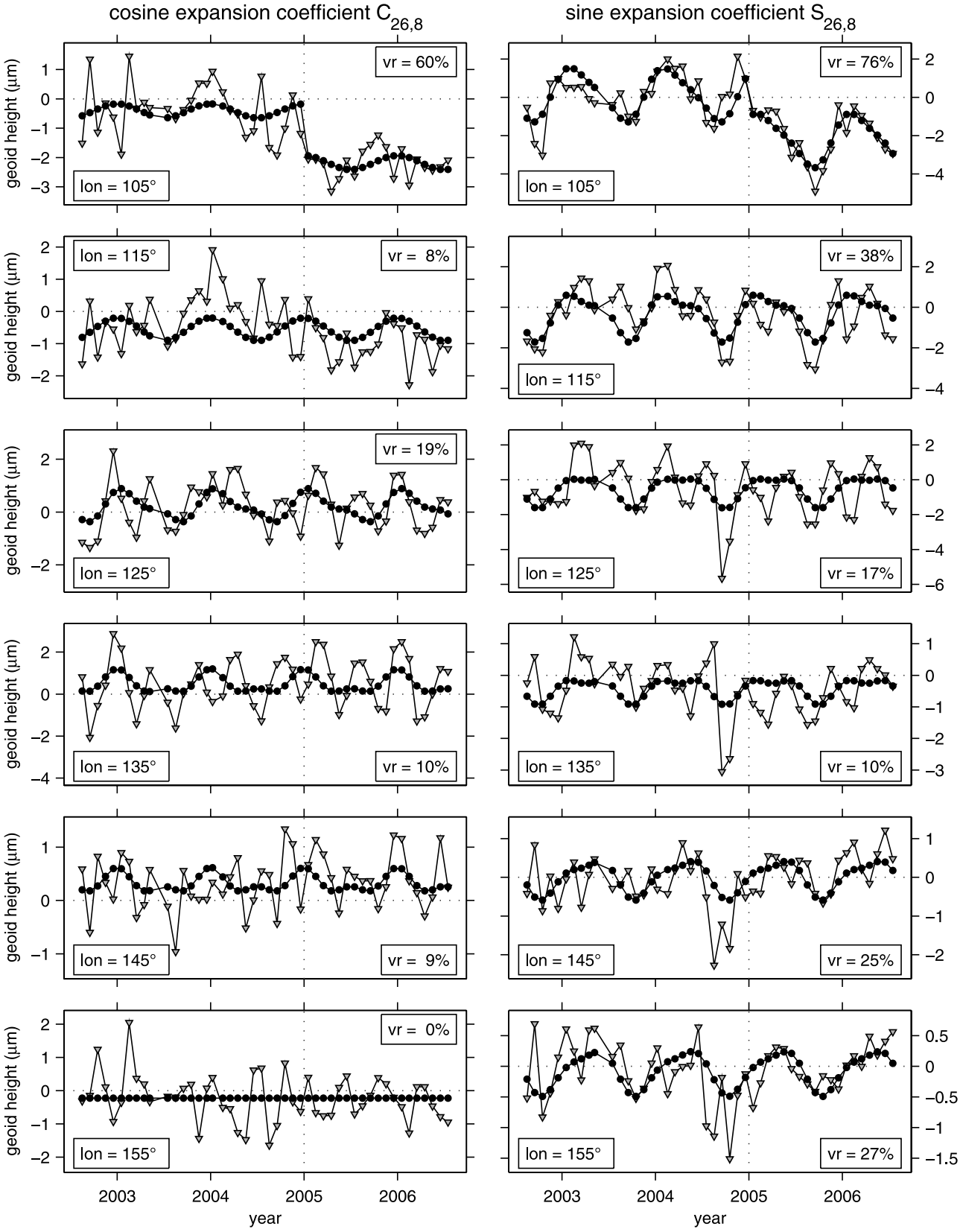

Figure 5. Time series of the tapered GRACE geopotential coefficients of degree 26 and order 8 after applying window functions located at various centers away from the epicenter of the Sumatra-Andaman earthquake, at 5°N and 105°E, 115°E, 125°E, 135°E, 145°E, and 155°E. Note that the localized GRACE coefficients may reveal signals other than those owing to the earthquake, because the window is positioned away from the epicenter.

resolved if each estimate is statistically significant (i.e., if the t value of the estimate, which is computed by taking the ratio of the parameter estimate and its standard error estimate, exceeds 1 to give 70% of confidence) and the postfit variances are reduced to more than 80% by using either M2 or M3. Otherwise, the time series is considered to merely reflect a seasonal pattern that is well accounted for by M1. When both M2 and M3 yielded significant variance reduction, we compared them. The model (either M2 or M3) with the lowest postfit variance was chosen as representative of the time series. The linear trend and step function cannot be used simultaneously since they are anticorrelated significantly, especially if the data span is too short. That is, a positive linear trend and a negative step may compensate in a time series that requires neither. We do not rule out that longer data spans would allow us to separately resolve both a linear trend and a step change.

[17] In Figure 3, the analytic fits to some of the time series of individual SH coefficients after windowing are depicted and the variance reduction (vr) owing to the fits, in percent, is indicated. This is computed as the difference between one hundred and one hundred times the ratio of the variance of the postfit residuals to the variance of the original data. In the time series, the seasonal pattern was readily evident. Figure 3 also shows how abrupt stepwise coseismic changes associated with the earthquake are to be found in many of the tapered coefficient series, if not in all of them. Owing to the offset in plotting the results, the height of the step (though not whether it is statistically significant) before and after the earthquake can be read off the axes. The seasonal pattern and its yearly change (the interseasonal pattern) are large for the low-degree harmonics which renders any coseismic change relatively unobservable. We postpone a discussion on the inversion results for the coseismic change to a later section.

[18] For comparison, we depict the results of identical modeling on the original unwindowed "global" GRACE solutions in Figure 4. The magnitude of the time-variable gravity fluctuation is more than one order of magnitude larger than the windowed coefficients of Figure 3. No coseismic change is evident in the time series except perhaps for a minute one for low-degree coefficients such as $C_{4,4}$. In the time series of the coefficients $C_{43,14}$ and $S_{43,14}$, there is no significant fit (indicated by straight line) with any of aforementioned models. Comparing Figures 3 and 4 we infer that the SNR of the earthquake signal was indeed greatly improved by windowing. The energy of the earthquake signal is concentrated inside of the windowed region and decays quickly outside of it, whereas the GRACE errors are rather uniform over the entire globe, as we saw previously from the degree-RMS of fields windowed about various locations (Figure 1b). The globally averaged energy of the coseismic signal is too small to be picked up above the noise level. Analyzed with a suitably band-limited and regionally concentrated window, the time series of GRACE coefficients are cleaned up to reveal the underlying subtle gravity change that can be attributed to the Sumatra-Andaman earthquake. It is not the purpose of this paper to explore in detail the error structure of GRACE-derived time series of gravity change coefficients (random and correlated errors as reported by *Swenson and Wahr* [2006], possibly due to mismodeled temporal signal as well as instrumental noise) nor to derive windowing functions that would take this into account; this has been proposed and carried out by *Swenson and Wahr* [2002]. Rather, we have highlighted the raw power of spatiospectral concentration to extract local contributions from global SH time series. In the following section, we use the data obtained via our procedure outlined above to study the coseismic gravity change owing to the Sumatra-Andaman earthquake in more detail.

[19] For completeness, we applied the same shape window function to the GRACE fields, but centered at various different locations. The results are shown in Figure 5 for one particular harmonic coefficient pair ($C_{26,8}$ and $S_{26,8}$). The window has been moved from the Sumatra region eastward (from 5°N/95°E to 5°N/155°E). From the coefficients centered at 5°N/105°E that is, close to our region, shown in the top two panels of Figure 5, the coseismic signal is still found but with smaller magnitude than the one windowed at the right place shown on the third row of panels of Figure 3. However, there was no such abrupt jump found from the windowed coefficients centered at other places. Interestingly, a peculiar periodic pattern is found around the Indonesian islands and north of Papua New Guinea (shown in the third and fourth rows of panels with longitude of 125°E and 135°E), which is characterized by a period of 161 days indicating residual S_2 ocean tides [*Ray et al.*, 2003].

4. Inference of Coseismic Gravity Change

[20] The best fitting cosine and sine SH coefficients of the step function (offset by the earthquake) of each time series of the windowed GRACE coefficients up to degree and order 55 were estimated and tested for their statistical significance. The mean amplitudes for each degree and order, defined as $\sqrt{\left(C_{lm}^2 + S_{lm}^2\right)/2}$, of the significant estimates of the coseismic jump are depicted in Figure 6a. White areas in the range $m \leq l$ indicate estimates that are not statistically significant. The larger changes shown with warmer colors in the range of $>10^{-12}$ are found mostly near the sectorial harmonic ($m = l$) coefficients. At the same degree, higher-order coefficients pick up larger coseismic offsets. We have computed the error estimates of such coseismic coefficient estimates by computing the postfit residuals about the applied model including the step function (M3). Figure 6b depicts the error estimates that are approximately several factors to an order magnitude smaller than the amplitude of the signals.

[21] The gravity change predicted by *Han et al.* [2006, Figure S3] is shown for comparison in Figure 6c. The result of this seismic model prediction, although it is a planar elastic half-space model [*Okada*, 1992], was expanded into SH coefficients by numerical quadrature up to degree and order 360 and subsequently tapered using the same window function used to process the GRACE coefficients. The mean amplitude of the predicted coseismic change is depicted in Figure 6c; its intensity may be directly compared with the estimates derived from GRACE. Our windowing procedure has introduced stabilizing local correlations between the estimates at different degrees for any given order. Hence the individual estimates at a particular degree and order are by

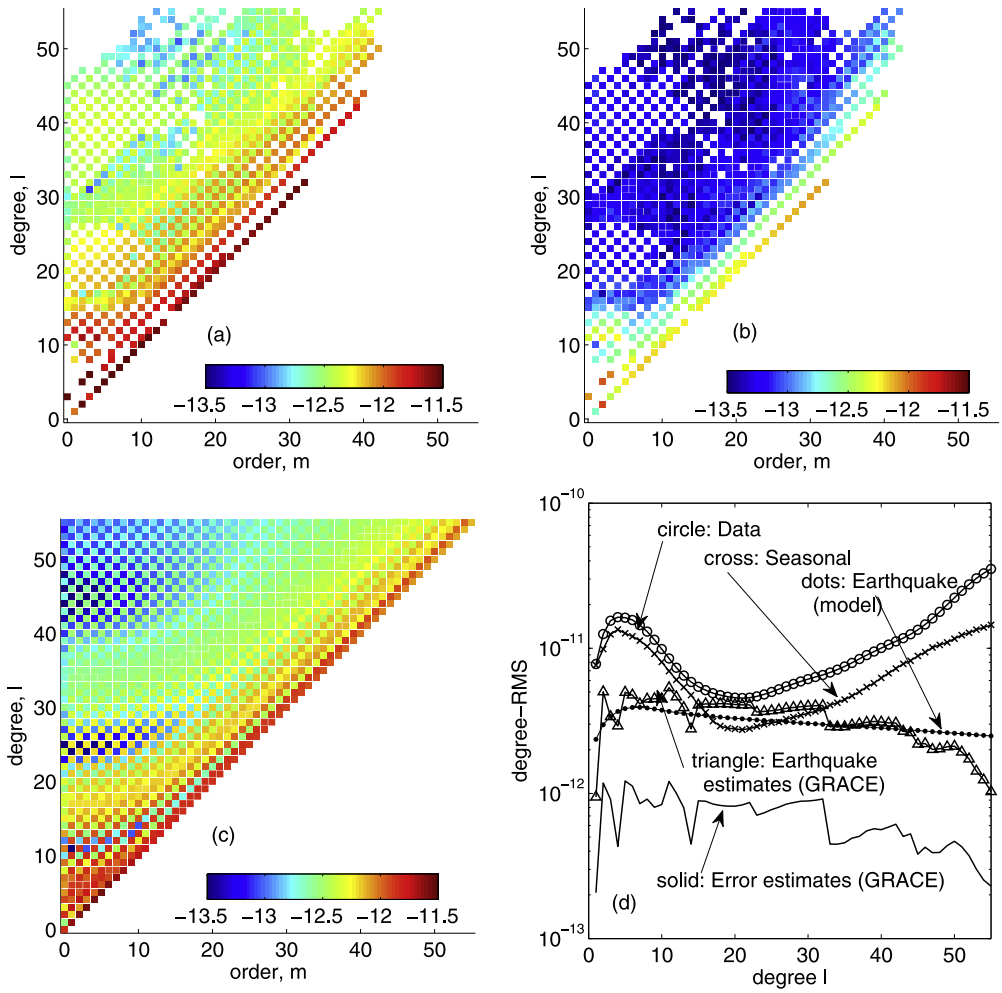

Figure 6. (a) Mean amplitude of the coseismic coefficients estimated from the windowed GRACE time series. Note that not all coefficients show significant nonzero coseismic jumps in the time series. White areas ($m \leq l$) indicate that the time series at that particular degree and order do not produce any statistically significant jump. (b) Mean amplitude of the error estimates of coseismic coefficients. (c) Mean amplitude of the coefficients indicating the coseismic change predicted from the seismic model, windowed identically to the observations. (d) The root-mean-squared energy per degree (degree-RMS) of the seasonal component and coseismic change estimates and error estimates for the coseismic coefficients from the windowed GRACE time series; the degree-RMS of the predicted coseismic signal; and the degree-RMS of the windowed GRACE time series indicating the strength of the data.

no means statistically independent. However, by windowing the results of the predicted gravity change in a manner analogous to the observations, we are justified in making model comparisons. The very low-degree ($l \leq 9$) components of the coseismic change are not well recovered from GRACE except when the sectorial harmonics are con cerned. However, the observations and predictions are generally in good agreement.

[22] Figure 6d presents the time-averaged degree-RMS of the GRACE observations, the degree-RMS of the estimated seasonal (annual + semiannual) variation, the estimated coseismic change and its error estimate, and the coseismic change predicted from the earthquake model, all after windowing with the same function. The overall magnitudes of the coseismic changes estimated from GRACE coefficients are in agreement with the ones predicted from the seismic model. We observe that the power of the seasonal estimates is much stronger at low degrees ($l \leq 10$) and rapidly decays before growing gradually again after degree 20. The growing power beyond degree 20 may well be attributed to error. However, the coseismic component shows relatively flat spectral energy larger than the seasonal component when the degree is larger than 15. If we calculate the seasonal and coseismic estimates with tighter significance level, for example, with a t value of 3 indicating >99% confidence, this component of error in the seasonal estimates is greatly reduced and the spectral energy decays faster with increasing degree. However, using greater t values loses some of the useful information in the coseismic estimates. We tested various t values to obtain the closest fit between GRACE-derived and seismically predicted degree-RMS values. Using a t value of 1, i.e., for a 70% confidence level, yields the most plausible results

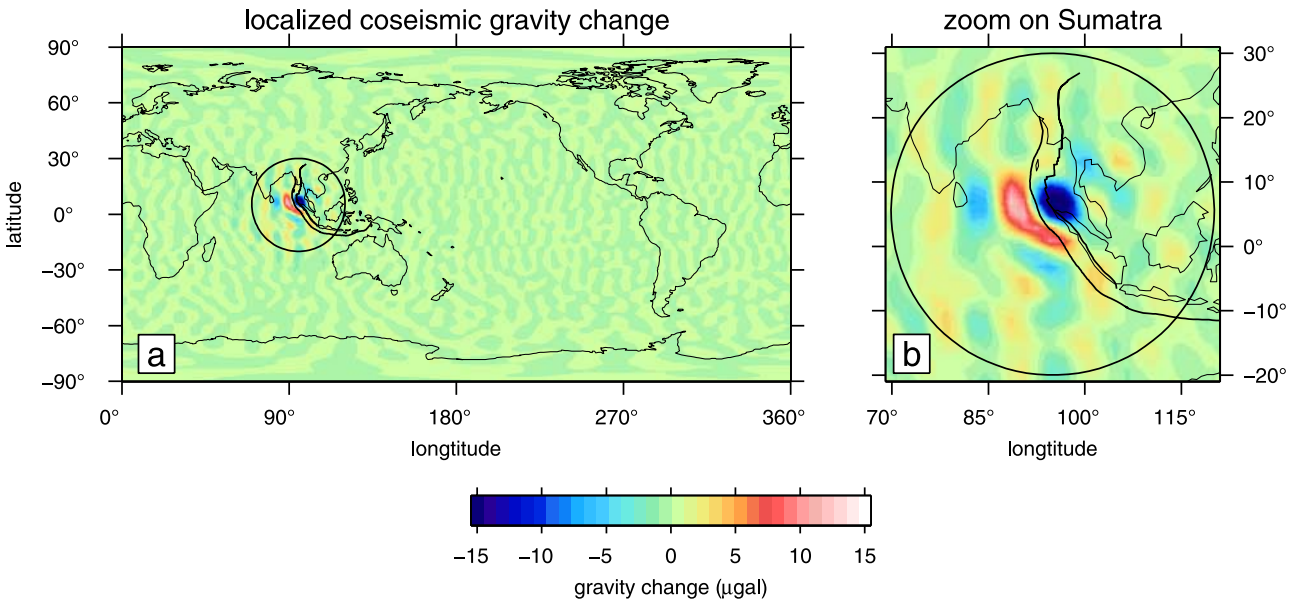

Figure 7. (a) The coseismic gravity change (μGal) expanded from the sizes of the jumps in the time series of the localized coefficients up to degree and order 55. (b) The same as Figure 7a zoomed in on our region of interest.

on the basis of the comparison between observed and predicted degree-RMS of the coseismic change.

[23] The spatial distribution of the coseismic gravity anomaly was calculated from the estimated coseismic jumps from each of the windowed GRACE SH time series; this is shown in Figure 7. Only nonzero estimates up to degree and order 55 were used. The calculated anomaly follows the Java trench fairly well, yielding positive gravity anomalies west and negative anomalies (with larger magnitude) east of the trench. Gravity fluctuations outside of the spherical cap generally do not exceed ±1 μGal. From the order-lumped power spectra comparison between the coseismic signal and error estimates shown in Figure 6d, it is indicated that the errors have roughly 25 times less power (or 5 time less variability) than the signal at all frequencies. We further obtain a 2–3 μGal error estimate of the coseismic gravity changes shown in Figure 7b. Also note that there are still north-south elongated stripes with $\pm\sim$3 μGal variation in the windowed gravity map which are likely due to correlated errors especially existing in resonant orders, as reported by *Han et al.* [2004] on the basis of simulations and by *Swenson and Wahr* [2006] from actual GRACE data processing.

[24] Other than comparing power or intensity, we also compared the GRACE estimates with the seismic model predictions by calculating the degree-correlation coefficient γ_l [e.g., *Arkani-Hamed*, 1998] between the two sets of windowed SH expansion coefficients, as follows:

$$\gamma_l = \frac{\sum_{m=0}^{l}\left\{C_{lm}^{GRACE}C_{lm}^{Seis} + S_{lm}^{GRACE}S_{lm}^{Seis}\right\}}{\sqrt{\sum_{m=0}^{l}\left\{\left(C_{lm}^{GRACE}\right)^2+\left(S_{lm}^{GRACE}\right)^2\right\}}\sqrt{\sum_{m=0}^{l}\left\{\left(C_{lm}^{Seis}\right)^2+\left(S_{lm}^{Seis}\right)^2\right\}}}, \quad (9)$$

where C_{lm}^{GRACE} and S_{lm}^{GRACE} are the coseismic coefficients estimated from GRACE time series and C_{lm}^{Seis} and S_{lm}^{Seis} are the ones predicted from the seismic model. As *Han et al.* [2006], we now consider two components of the total gravity effect (Figure 8a) that can be seismically predicted separately, namely the changes caused by the vertical displacement at the seafloor and Moho (Figure 8b) and the density change within the crust and mantle (Figure 8c). Once again, we used a spherical harmonic expansion up to degree and order 55 after applying the spectral convolution with the window function. Figure 8d shows the degree-dependent correlation coefficients between the GRACE observations and the model predictions. Most of all GRACE SH coseismic coefficients are in very good agreement with the model prediction, showing positive correlations greater than 0.8. The higher-degree harmonics ($l \geq 30$) of the observations are especially well correlated with the effects owing to vertical displacement as shown in Figure 8b. The lower-degree GRACE coefficients are mostly correlated with the effects caused by the density change as shown in Figure 8c. These findings agree with the conclusions reached by re-analyzing the over-flight GRACE tracking data directly [*Han et al.*, 2006], which, as we emphasize again, involved much more laborious processing.

[25] Aside from the solid-Earth effects that can be robustly attributed to the Sumatra-Andaman earthquake, the second significant pattern to emerge from the windowed time series are the seasonal (mostly annual) fluctuations. To illustrate this, we calculated the coefficients of the gravity changes modeled with the in-phase (sine) and out-of-phase (cosine) annual sinusoids from the windowed GRACE SH coefficients series and depicted them in Figures 9a and 9b. A maximum degree and order to 20 has been maintained to minimize the effects caused by increasing power in the ill-determined higher-degree and order coefficients (see the discussion surrounding Figure 6c). Large variations are

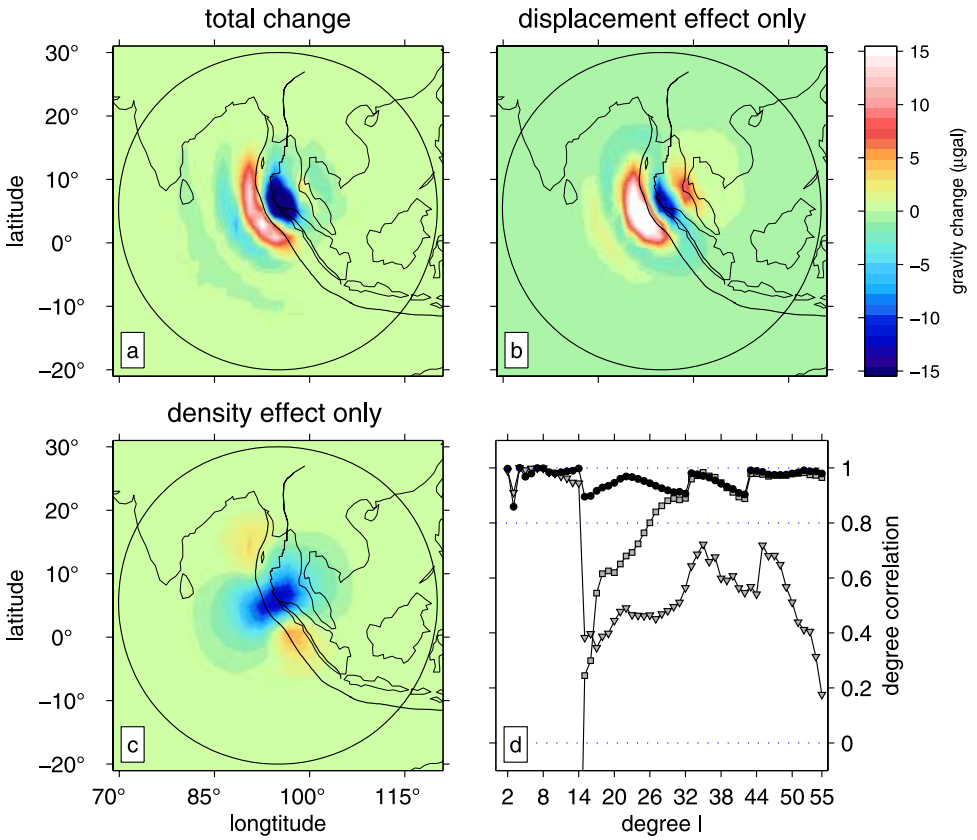

Figure 8. (a) The (total) coseismic gravity change (μGal) predicted from the seismic model. (b) The gravity change caused only by the predicted vertical displacement of the seafloor and Moho. (c) The gravity change caused only by the predicted density change in the crust and mantle. (See *Han et al.* [2006] for a detailed description of the earthquake model.) Note that Figure 8a equals 8b plus 8c. A spherical harmonic expansion up to degree and order 55 has been used. (d) Degree-correlation coefficients between the GRACE estimates and the model coefficients, depicted by black circles, gray squares, and gray triangles, for Figures 8a–8c, respectively. Note that each of the gravity effects correlates with the GRACE observations in distinct harmonic degrees. The correlations of the vertical displacement at low degrees are negative, and hence off the scale.

observed over land and within the spherical cap, and contained in the in-phase component. Although large seasonal variations are expected (recording hydrological cycles) in Bangladesh and surrounding areas, most of these are strongly diminished by windowing. For comparison, we show terrestrial water storage changes averaged monthly from the Land Data Assimilation System (LDAS) model, developed at NOAA's Climate Prediction Center (CPC) (*Fan et al.* [2003]; see also www.csr.utexas.edu/research/ggfc). The available gridded data were decomposed into SH coefficients and windowed identically to the GRACE solutions. The in-phase and out-of-phase components of the LDAS/CPC model agree well with the GRACE estimates, as shown in Figures 9c and 9d.

5. Discussion and Conclusions

[26] We analyzed 45 time series of monthly geopotential spherical harmonic coefficients from the GRACE mission by means of spatiospectral localization. This improves the signal-to-noise ratio in the coefficients and recovers the gravity change associated with the great Sumatra-Andaman earthquake. The localization amounts to the spectral convolution of the GRACE harmonics with the response of an optimally concentrated band-limited window centered around the earthquake region. The effect of the globally uniform measurement errors in the GRACE coefficients has been reduced by localization and consequently any intense signal that is regionally confined to the region of interest can be better identified from the coefficients. The 2004 great Sumatra-Andaman earthquake significantly broke the time series of many of the global spherical harmonic coefficients below degree and order 55, which can be seen only after localizing the global coefficients at the right place (i.e., around the epicenter). The amount of the abrupt change after the earthquake in each of the time series of GRACE coefficients is in the range of 1–10 μm geoid height, and, when summed over all orders at each degree (the degree-RMS), about ten times larger. Although such values are well below the expected error degree-RMS of the monthly global GRACE spectra, they are identifiable after localization.

[27] Most of the coseismic changes in the coefficients resolved by localizing GRACE solutions agree well with a

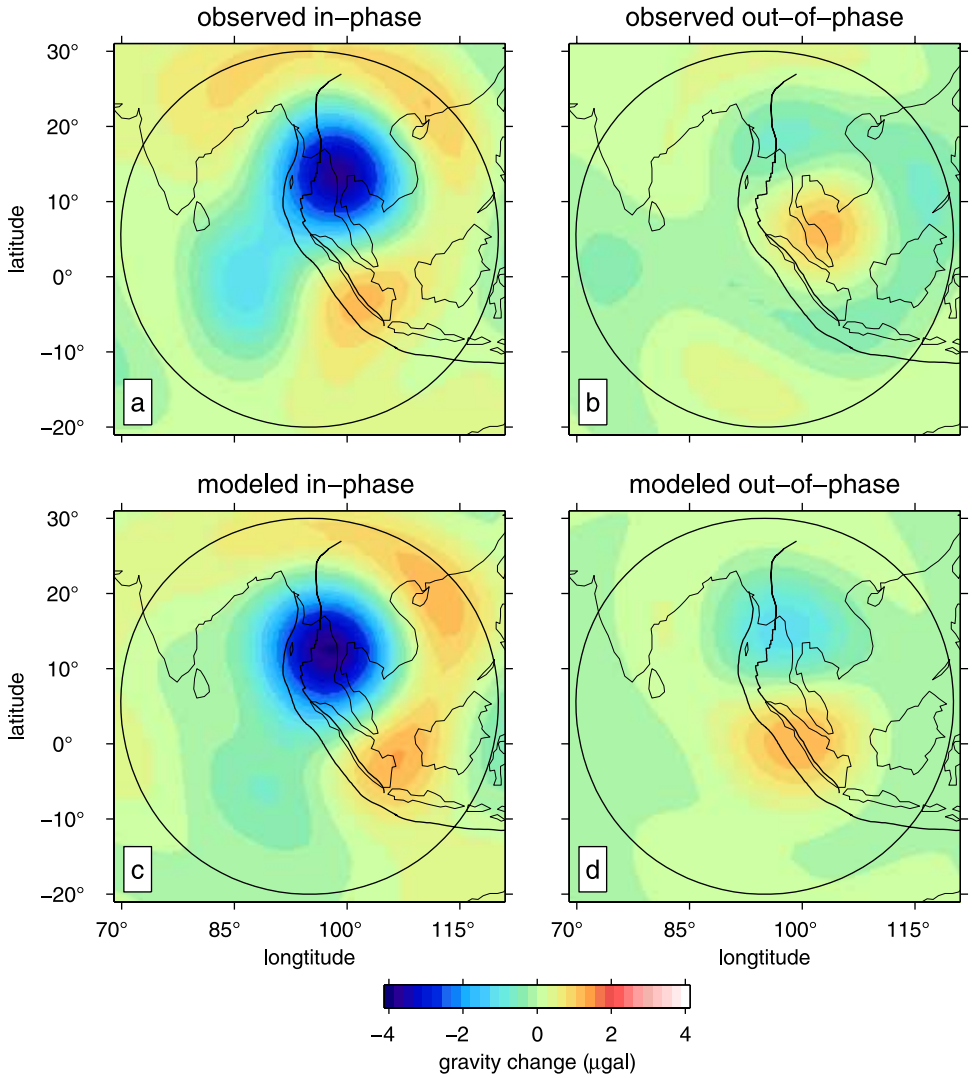

Figure 9. (a and b) Maps produced by expanding the coefficients of in-phase (sine) and out-of-phase annual (cosine) gravity variations (μGal), respectively, estimated from the windowed GRACE coefficients up to degree and order 20. Note that the greatest annual variability is over the continents and limited to the inside of the spherical cap. The large variability expected in Bangladesh, which is not the subject of this paper, has been diminished by windowing. (c and d) The same as Figures 9a and 9b, but predicted from the windowed SH coefficients of the land data assimilation system (LDAS).

seismic model in terms of both intensity and correlation up to degree and order 55. Many of the higher-degree components ($l \geq 30$) are best correlated with the effect caused by vertical displacement due to the earthquake, while the lower-degree components most closely match the effects of the predicted density change. Both GRACE observations and the model predictions yield around 30 μGal peak-to-peak gravity changes around the Andaman Sea.

[28] The method and results shown in this study show the great potential of the analysis of time-variable gravity fields by localization of global spherical harmonic solutions. While these are often very noisy, they contain regional contributions from specific geographical areas that are easily identifiable after spatiospectral localization. The coseismic signal from the spatiospectral localization of monthly geopotential coefficient estimates is comparable to the one from localized analysis of direct satellite tracking data in strength and spatial resolution.

[29] The observed coseismic gravity change due to the undersea earthquake extends out to the ocean, where we suffer from lack of direct geodetic or seismic measurements. A vast amount of signal originates here, which may be useful to constrain earthquake source parameters even though the gravitational observables are limited to large spatial scale (a few hundreds km). The lack of observations right above the rupture plane (i.e., above ocean) results in the well-known trade-off between total seismic moment and fault dip [*Kanamori and Given*, 1981; *Banerjee et al.*, 2005]. The GRACE gravity estimates with accuracy of 2–3 μGal on top of the rupture plane with homogeneous coverage and accuracy may be useful to resolve the dip angles of fault planes of shallow subduction earthquakes, as we plan to investigate in forthcoming work.

[30] **Acknowledgments.** This work was supported by the NASA Gravity Recovery and Climate Experiment (GRACE) project. We acknowledge the NASA/GFZ GRACE project for the GRACE data products (distributed by the Jet Propulsion Laboratory Physical Oceanography Distributed Active Archive Center (JPL PODAAC)). F. J. S. was supported by a Natural Environment Research Council Young Investigators' Award (NE/D521449/1) and a Nuffield Foundation grant for Newly Appointed Lecturers (NAL/01087/G) while at University College London, and by National Science Foundation grants EAR-0710860 and EAR-0105387 while at Princeton University. Matlab routines can be obtained from www.frederik.net. We furthermore thank Mark Wieczorek for providing the FORTRAN codes for this work via the web site (www.ipgp.jussieu.fr/~wieczor/SHTOOLS) and Chen Ji for providing his coseismic slip model of the 2004 Sumatra-Andaman earthquake.

References

Ammon, C., et al. (2005), Rupture process of the 2004 Sumatra-Andaman earthquake, *Science*, *308*, 1133–1139.

Arkani-Hamed, J. (1998), The lunar mascons revisited, *J. Geophys. Res.*, *103*, 3709–3739.

Banerjee, P., et al. (2005), The size and duration of the Sumatra-Andaman earthquake from far-field static offsets, *Science*, *308*, 1769–1772.

Chambers, D. P., J. Wahr, and R. S. Nerem (2004), Preliminary observations of global ocean mass variations with GRACE, *Geophys. Res. Lett.*, *31*, L13310, doi:10.1029/2004GL020461.

Dahlen, F. A., and J. Tromp (1998), *Theoretical Global Seismology*, Princeton Univ. Press, Princeton, N. J.

Davis, J. L., P. Elósegui, J. X. Mitrovica, and M. E. Tamisiea (2004), Climate-driven deformation of the solid Earth from GRACE and GPS, *Geophys. Res. Lett.*, *31*, L24605, doi:10.1029/2004GL021435.

Fan, Y., H. Van den Dool, K. Mitchell, and D. Lohmann (2003), A 51-year reanalysis of the U.S. land-surface hydrology, *GEWEX Newsl.*, *13*, 6–10.

Freeden, W., and V. Michel (1999), Constructive approximation and numerical methods in geodetic research today—An attempt at a categorization based on an uncertainty principle, *J. Geod.*, *73*, 452–465.

Han, S.-C., C. Jekeli, and C. K. Shum (2004), Time-variable aliasing effects of ocean tides, atmosphere, and continental water mass on monthly mean GRACE gravity field, *J. Geophys. Res.*, *109*, B04403, doi:10.1029/2003JB002501.

Han, S.-C., et al. (2005), Non-isotropic filtering of GRACE temporal gravity for geophysical signal enhancement, *Geophys. J. Int.*, *163*, 18–25, doi:10.1111/j.1365-246X.2005.02756.x.

Han, S.-C., C. K. Shum, M. Bevis, C. Ji, and C.-Y. Kuo (2006), Crustal dilatation observed by GRACE after the 2004 Sumatra-Andaman earthquake, *Science*, *313*, 658–662, doi:10.1126/science.1128661.

Kanamori, H., and J. W. Given (1981), Use of long-period surface-waves for rapid-determination of earthquake-source parameters, *Phys. Earth Planet. Inter.*, *27*, 8–31.

Kusche, J. (2007), Approximate decorrelation and non-isotropic smoothing of time-variable GRACE-type gravity field models, *J. Geod.*, *81*(11), 733–749, doi:10.1007/s00190-007-0143-3.

Luthcke, S. B., H. J. Zwally, W. Abdalati, D. D. Rowlands, R. D. Ray, R. S. Nerem, F. G. Lemoine, J. J. McCarthy, and D. S. Chinn (2006), Recent Greenland ice mass loss by drainage system from satellite gravity observations, *Science*, *314*, 1286–1289, doi:10.1126/science.1130776.

Okada, Y. (1992), Internal deformation due to shear and tensile faults in a half-space, *Bull. Seismol. Soc. Am.*, *82*, 1018–1040.

Okubo, S. (1992), Gravity and potential changes due to shear and tensile faults in a half-space, *J. Geophys. Res.*, *97*, 7137–7144.

Percival, D. B., and A. T. Walden (1993), *Spectral Analysis for Physical Applications, Multitaper and Conventional Univariate Techniques*, Cambridge Univ. Press, New York.

Ray, R. D., D. D. Rowlands, and G. D. Egbert (2003), Tidal models in a new era of satellite gravimetry, *Space Sci. Rev.*, *108*, 271–282.

Sabadini, R., G. Dalla Via, M. Hoogland, and A. Aoudia (2005), A Splash in Earth Gravity from the 2004 Sumatra Earthquake, *Eos Trans. AGU*, *86*(15), 149.

Simons, F. J., and F. A. Dahlen (2006), Spherical Slepian functions and the polar gap in geodesy, *Geophys. J. Int.*, *166*, 1039–1061, doi:10.1111/j.1365-246X.2006.03065.x.

Simons, F. J., F. A. Dahlen, and M. A. Wieczorek (2006), Spatiospectral concentration on a sphere, *SIAM Rev.*, *48*, 504–536, doi:10.1137/S0036144504445765.

Simons, M., and B. H. Hager (1997), Localization of the gravity field and the signature of glacial rebound, *Nature*, *390*, 500–504.

Simons, M., S. Solomon, and B. H. Hager (1997), Localization of gravity and topography: Constraints on the tectonics and mantle dynamics of Venus, *Geophys. J. Int.*, *131*, 24–44.

Swenson, S., and J. Wahr (2002), Methods for inferring regional surface-mass anomalies from Gravity Recovery and Climate Experiment (GRACE) measurements of time-variable gravity, *J. Geophys. Res.*, *107*(B9), 2193, doi:10.1029/2001JB000576.

Swenson, S., and J. Wahr (2006), Post-processing removal of correlated errors in GRACE data, *Geophys. Res. Lett.*, *33*, L08402, doi:10.1029/2005GL025285.

Tapley, B. D., and C. Reigber (2005), The GRACE mission, status, results and projections, paper presented at GRACE Science Team Meeting, Univ. of Tex., Austin, Tex., 13–14 Oct.

Tapley, B. D., S. Bettadpur, M. Watkins, and C. Reigber (2004a), The gravity recovery and climate experiment: Mission overview and early results, *Geophys. Res. Lett.*, *31*, L09607, doi:10.1029/2004GL019920.

Tapley, B. D., S. Bettadpur, J. Ries, P. Thompson, and M. Watkins (2004b), GRACE Measurements of mass variability in the Earth system, *Science*, *305*, 503–505.

Velicogna, I., and J. Wahr (2006), Measurements of time-variable gravity show mass loss in Antarctica, *Science*, *311*, 1754–1756.

Wahr, J., F. Molenaar, and F. Bryan (1998), Time variability of the Earth's gravity field: Hydrological and oceanic effects and their possible detection using GRACE, *J. Geophys. Res.*, *103*, 30,205–30,229.

Wieczorek, M. A., and F. J. Simons (2005), Localized spectral analysis on the sphere, *Geophys. J. Int.*, *162*, 655–675, doi:10.1111/j.1365-246X.2005.02687.x.

S.-C. Han, Planetary Geodynamics Laboratory, Code 698, NASA Goddard Space Flight Center, Greenbelt, MD 20771, USA. (schan@puuoo.gsfc.nasa.gov)

F. J. Simons, Department of Geosciences, Princeton University, Guyot Hall, Princeton, NJ 08544, USA. (fjsimons@alum.mit.edu)